Removing trailing tails and delays induced by artificial dissipation in Padé numerical schemes for stable compacton collisions

Julio Garralón, Francisco Rus, Francisco R. Villatoro*

Dept. Lenguajes y Ciencias de la Computación, Universidad de Málaga, 29071 Málaga, Spain

Abstract

The numerical simulation of colliding solitary waves with compact support arising from the Rosenau–Hyman K(n, n) equation requires the addition of artificial dissipation for stability in the majority of methods. The price to pay is the appearance of trailing tails, amplitude damping, and delays as the solution evolves. These undesirable effects can be corrected by properly counterbalancing two sources of artificial dissipation; this procedure is designed by using the slow time evolution of the parameters of the solitary waves under the presence of the dissipation determined by means of adiabatic perturbation methods. The validity of the tail removal methodology is demonstrated on a Padé numerical scheme. The tails are completely removed leaving only a small compact ripple at the original position of their front, and the numerical stability of the scheme under compacton collisions is preserved, as shown by extensive numerical experiments for several values of n.

Keywords:

Solitary waves, Compactons, Adiabatic perturbations, Artificial viscosity, Numerical methods, Padé approximants, Nonlinear evolution equations

^{*}Corresponding author. Tel.: 34-951952388; fax: +34-951952542. E-mail address: villa@lcc.uma.es

1. Introduction

Rosenau and Hyman [1] came across solitary waves with compact support, therein referred to as *compactons*, while studying the nonlinear dispersion in the formation of patterns in liquid drops. These traveling waves arose as solutions of a particular generalization of the well-known Korteweg–de Vries equation, commonly denoted as K(m, n), that reads

$$u_t + (u^m)_x + (u^n)_{xxx} = 0, \qquad m > 0, \quad 1 < n \le 3, \tag{1}$$

where u(x, t) is the wave amplitude as a function of the spatial variable x, and time t. Current analytical studies of this equation [2, 3, 4, 5, 6, 7, 8, 9], cannot deal with the interaction between compactons. Hence, numerical methods, such as pseudospectral schemes [1, 10], finite elements [11, 12], finite differences [11, 13], Padé approximants [14, 15], modified equations [16] or particle schemes based on the dispersive-velocity method [17], must be used.

The majority of the numerical methods for compacton equations require the addition of artificial viscosity in order to cope with collisions, since otherwise instabilities appear which may cause a blow up in the solution. In pseudospectral schemes a hyperviscosity term is used where a second-order, linear dissipative term affects only the high-frequency modes of the solution by using a high-pass filter [10]. In both finite element and finite difference schemes a fourth-order, linear dissipative term is frequently incorporated [11, 12, 13, 15, 16]. The addition of artificial viscosity in Eq. (1) distorts the original compacton, generating small trailing tails, amplitude damping and velocity losses. The development of a method for the numerical stabilization of the compactons in collisions without the appearance of tails is an open problem to be addressed in this paper.

Numerically-induced phenomena can be studied and corrected by means of the method of modified equations [16, 18]. For the analysis of these phenomena, perturbation methods [19] can be applied to the analysis of effects introduced by local truncation errors as perturbations of the original evolution equation. These methods have been successfully applied to ordinary differential equations [18, 20] and nonlinear evolution equations [21, 22, 23]. For compacton equations, adiabatic perturbation methods have been considered for the K(n, n) equation in Garralón and Villatoro [24], extending previous results for the n = 2 case in Pikovsky and Rosenau [25], and Rus and Villatoro [26]. These techniques, which generalize previous results for solitons [27, 28, 29], can be used to analytically determine the trailing tails introduced by the artificial viscosity, opening the possibility of their removal by means of correction terms modifying the original evolution equation.

In this paper adiabatic perturbation methods are applied to the K(n, n) equation and a new numerical technique for trailing tail removal is introduced. The validity of this procedure is checked by means of a Padé numerical method. Section 2 is devoted to the development of the tail removal technique based on the adiabatic perturbation to the numerical scheme with artificial viscosity. In section 3 we briefly present the numerical method based on Padé approximants used to solve the K(n, n) equation. The results of extensive numerical experiments are presented in Section 4 for several values of n. Final conclusions are summarized in Section 5.

2. Adiabatic perturbations

The adiabatic perturbation method is applied to the K(n, n) equation with both second- and fourth-order linear dissipations. Such a method determines the slow time evolution of the parameters of the compactly supported solitary waves by using that of the invariants under the dissipative perturbation.

Let us consider the perturbed K(n, n) equation given by

$$u_t + (u^n)_x + (u^n)_{xxx} = \varepsilon \mathcal{P}(u), \qquad (2)$$

where $1 < n \leq 3$, the perturbation $\mathcal{P}(u)$ is a function of u and its spatial and temporal derivatives, and $|\varepsilon| \ll 1$ is a small parameter. After multiplying Eq. (2) by u^n and integrating in space, the only non-null term in its left-hand side is the first one, resulting in

$$\frac{d}{dt} \int_{-\infty}^{\infty} \frac{u^{n+1}}{n+1} \, dx = \varepsilon \, \int_{-\infty}^{\infty} u^n \, \mathcal{P}(u) \, dx, \tag{3}$$

whose left-hand side is the temporal derivative of the second invariant of the unperturbed K(n, n), i.e., exactly nil for Eq. (2) with $\varepsilon = 0$. However, perturbations such that the right-hand side of Eq. (3) is non-zero result in the adiabatic evolution of parameters of the compacton solution of the unperturbed equation. Introducing the slow time scale $\tau = \epsilon t$, the compacton solution of the K(n, n) can be written as

$$u_c(x,t,\tau) = \left\{ \frac{2 n c(\tau)}{n+1} \cos^2\left(\frac{n-1}{2 n} \left(x - c(\tau) t\right)\right) \right\}^{1/(n-1)}, \qquad (4)$$

for $|x - c(\tau)t| \leq n\pi/(n-1)$, and $u_c(x,t,\tau) = 0$ otherwise. Inserting this ansatz into the perturbed equation (3) the slow time evolution of the velocity $c(\tau)$ of the perturbed compacton can be calculated; note that the amplitude of the perturbed compacton is uniquely determined by this velocity.

Let us determine the evolution of $c(\tau)$ for perturbation given by

$$\varepsilon \mathcal{P}(u) = \alpha_2 \ u_{xx} - \alpha_4 \ u_{xxxx},\tag{5}$$

where $|\alpha_2|, |\alpha_4| \ll 1$ are small parameters; this perturbation is dissipative if $\alpha_2 > 0$ and $\alpha_4 > 0$. The substitution of Eqs. (5) and (4) into Eq. (3) yields an ordinary differential equation for $c(\tau)$ written as

$$c'(\tau) = -\frac{(n-1)^2}{n(n+3)} \alpha_2 \ c(\tau) - \frac{(n-1)^3 ((n-3)n-1)}{(n-5)n^3 (n+3)} \alpha_4 \ c(\tau).$$
(6)

The solution of this equation is

$$c(\tau) = c(0) \exp\left(-\frac{(n-1)^2}{n(n+3)}\alpha_2\tau - \frac{(n-1)^3((n-3)n-1)}{(n-5)n^3(n+3)}\alpha_4\tau\right), \quad (7)$$

showing that, under the perturbation, the velocity, as well as the amplitude, decays and produces lags compared with the unperturbed compacton.

The perturbation (5) introduces trailing tails in the perturbed compacton not accounted for by the ansatz (4), since the perturbed equation does not possess solitary waves solutions; hence the amplitude of the initial pulse slowly decays as described by Eq. (7). This decay results in the formation of a plateau behind the compacton; this behaviour is similar to that of the solitons of the Korteweg–de Vries equation under the same kind of perturbation [28]. Let us note that the adiabatic perturbation method can be used to estimate the shape of this tail, as shown in Refs. [25] and [26] for the K(2, 2) equation, and Ref. [24] for the K(n, n) equation.

The main contribution of this paper is the introduction of a new procedure for removing the trailing tail by properly adjusting the values of the small parameters α_2 and α_4 , suggested by the fact that their contributions in Eq. (5) have opposite signs. Fixing the value of α_2 as a function of α_4 and n yields

$$\alpha_2(n,\alpha_4) = -\frac{(n-1)\left((n-3)n-1\right)}{(n-5)n^2}\alpha_4.$$
(8)

For $1 < n \leq 3$, the value of $\alpha_2(n, \alpha_4)/\alpha_4$ is positive, increasing from 1/9 to 1/4 as *n* decreases from 3 to 2, and decreasing from 1/4 to 0 as *n* decreases from 2 to 1.

3. The numerical method

The tail removal procedure presented in the previous section could be incorporated into a numerical method for Eq. (1) which uses artificial viscosity in order to deal with compactons collisions. Obviously, this procedure could introduce new instabilities. For illustration purposes, let us consider one of the most used methods for Eq. (1), a Padé approximation in space, with periodic boundary conditions in a finite interval [0, L], and a method of lines in time as described in [14, 15]. Equation (2) with perturbations (5) and a moving frame of reference with velocity c_0 is given by

$$Eq[u] \equiv u_t - c_0 u_x + (u^n)_x + (u^n)_{xxx} - \alpha_2 u_{xx} + \alpha_4 u_{xxxx} = 0.$$
(9)

The Padé method of this equation results in

$$\mathcal{A}(\mathbf{E})\frac{dU_j}{dt} - c_0 \mathcal{B}(\mathbf{E})U_j + \mathcal{B}(\mathbf{E})(U_j)^n + \mathcal{C}(\mathbf{E})(U_j)^n - \alpha_2 \mathcal{S}(\mathbf{E})U_j + \alpha_4 \mathcal{D}(\mathbf{E})U_j = 0, \qquad j = 0, 1, \dots M, \quad (10)$$

where the spatial grid nodes are $x_j = j \Delta x$, for $j = 0, 1, \ldots M$, with $\Delta x = L/M$, the numerical solution is $U_j(t) \approx u(x_j, t)$, the shift operator E is defined as E $U_j = U_{j+1}$, and $\mathcal{A}^{-1}(E) \mathcal{B}(E)$, $\mathcal{A}^{-1}(E) \mathcal{S}(E) \mathcal{A}^{-1}(E) \mathcal{C}(E)$, and $\mathcal{A}^{-1}(E) \mathcal{D}(E)$ are Padé operators for the first-, second-, third-, and fourthorder spatial derivatives respectively. Concretely, the Padé operators to be used in this paper are

$$\begin{aligned} \mathcal{A}(\mathbf{E}) &= \frac{\mathbf{E}^{-2} + 26 \, \mathbf{E}^{-1} + 66 + 26 \, \mathbf{E}^{1} + \mathbf{E}^{2}}{120} \\ \mathcal{B}(\mathbf{E}) &= \frac{- \, \mathbf{E}^{-2} - 10 \, \mathbf{E}^{-1} + 10 \, \mathbf{E}^{1} + \mathbf{E}^{2}}{24\Delta x}, \\ \mathcal{S}(\mathbf{E}) &= \frac{\mathbf{E}^{-2} + 2 \, \mathbf{E}^{-1} - 6 + 2 \, \mathbf{E}^{1} + \mathbf{E}^{2}}{6\Delta x^{2}}, \\ \mathcal{C}(\mathbf{E}) &= \frac{- \, \mathbf{E}^{-2} + 2 \, \mathbf{E}^{-1} - 2 \, \mathbf{E}^{1} + \mathbf{E}^{2}}{2\Delta x^{3}}, \end{aligned}$$

and

$$\mathcal{D}(\mathbf{E}) = \frac{\mathbf{E}^{-2} - 4 \,\mathbf{E}^{-1} + 6 - 4 \,\mathbf{E}^{1} + \mathbf{E}^{2}}{\Delta x^{4}},$$

corresponding to the following approximations to the first four spatial derivatives

$$\mathcal{A}^{-1}(\mathbf{E}) \,\mathcal{B}(\mathbf{E}) \,u(x_j, t) = \frac{\partial u}{\partial x}(x_j, t) + \frac{\Delta x^6}{5040} \frac{\partial^7 u}{\partial x^7}(x_j, t) + \mathcal{O}\left(\Delta x^8\right),$$
$$\mathcal{A}^{-1}(\mathbf{E}) \,\mathcal{S}(\mathbf{E}) \,u(x_j, t) = \frac{\partial^2 u}{\partial x^2}(x_j, t) + \frac{\Delta x^4}{720} \frac{\partial^6 u}{\partial x^6}(x_j, t) + \mathcal{O}\left(\Delta x^6\right),$$
$$\mathcal{A}^{-1}(\mathbf{E}) \,\mathcal{C}(\mathbf{E}) \,u(x_j, t) = \frac{\partial^3 u}{\partial x^3}(x_j, t) - \frac{\Delta x^4}{240} \frac{\partial^7 u}{\partial x^7}(x_j, t) + \mathcal{O}\left(\Delta x^6\right),$$

and

$$\mathcal{A}^{-1}(\mathbf{E}) \mathcal{D}(\mathbf{E}) u(x_j, t) = \frac{\partial^4 u}{\partial x^4}(x_j, t) - \frac{\Delta x^2}{12} \frac{\partial^6 u}{\partial x^6}(x_j, t) + \mathcal{O}\left(\Delta x^4\right).$$

The modified equation of the numerical method (10), which includes the local truncation error terms, is given by

$$Eq[u(x_j, t)] - \alpha_4 \frac{\Delta x^2}{12} \frac{\partial^6 u}{\partial x^6}(x_j, t) + O\left(\Delta x^4\right) = 0, \qquad (11)$$

showing that the numerical scheme is dissipative (for $\alpha_4 > 0$) after the application of the tail removal procedure.

For the discretization in time of Eq. (10), let us use the second-order accurate, implicit midpoint rule, yielding

$$\mathcal{A}(\mathbf{E})\frac{U_{j}^{(i+1)} - U_{j}^{(i)}}{\Delta t} - (c_{0}\mathcal{B}(\mathbf{E}) + \alpha_{2}\mathcal{S}(\mathbf{E}) - \alpha_{4}\mathcal{D}(\mathbf{E}))\frac{U_{j}^{(i+1)} + U_{j}^{(i)}}{2} + (\mathcal{B}(\mathbf{E}) + \mathcal{C}(\mathbf{E}))\left(\frac{U_{j}^{(i+1)} + U_{j}^{(i)}}{2}\right)^{n} = 0, \quad (12)$$

where Δt is the time step and $U_j^{(i)} \approx u(x_j, i \Delta t)$. The resulting nonlinear system of equations is solved for $U_j^{(i+1)}$ by using the Newton's iterative method.

4. Presentation of results

Let us study the behaviour of the new procedure for trailing tails removal on the compacton solutions of the K(n, n) equation with $n \in \{3, 2, 5/3, 3/2, 7/5, 4/3, 9/7, 5/4\}$. Numerical solutions with several values of α_4 will be compared with both $\alpha_2 = 0$ and $\alpha_2 = \alpha_2(n, \alpha_4)$, for the propagation of a one-compacton solution and for the collisions between two compactons.

4.1. One-compacton solutions

Let us first consider the evolution of a one-compacton solution with and without the tail removal procedure. Figure 1 shows snapshots of the numerical solution at the same instant of time for several values of n. The left plots show the trailing tails that appear when $\alpha_2 = 0$, for $\alpha_4 = 10^{-3}$ (top plot) and $\alpha_4 = 10^{-5}$ (bottom plot). Note that a zoom in has been used since the amplitude of the tails is several orders of magnitude smaller than that of the compacton. The tail starts at the initial location of the compacton at t = 0 with a ripple with a negative peak followed by a positive one; after the ripple, the tail has a nearly constant plateau connecting with the left edge of the compacton. The amplitude of the tail decreases as n does and as so does α_4 . The right plots show the removal of these tails when using $\alpha_2(n, \alpha_4)$, for $\alpha_4 = 10^{-3}$ (top plot) and $\alpha_4 = 10^{-5}$ (bottom plot). The plateau completely disappears, but the ripple in the tail front persists with smaller amplitude. In long-time integrations, the compacton is far away and clearly separated from the ripple located at its initial position, so it behaves as if there is no tail.

Figure 2 compares the evolution in time of the compacton maximum amplitude with $\alpha_2 = 0$ (dashed lines) and $\alpha_2(n, \alpha_4)$ (solid ones), i.e., with and without the tails. The appearance of the tails compensates the loss in the compacton maximum amplitude due to the dissipation since the first invariant is preserved during the propagation, hence, with the tail removal procedure, the maximum amplitude practically retains its initial value.

Table 1 shows the difference between the location of the analytical and numerical compacton maximum amplitudes at a time t = 2000 for several values of α_4 , with $\alpha_2 = 0$ and $\alpha_2(n, \alpha_4)$. The numerical velocity of the compactons in the dissipativeless case (when $\alpha_2 = \alpha_4 = 0$) is very near, but not exactly equal, to the analytical one, resulting in a very small difference in the position at t = 2000 of about 0.6 (for the values of Δx and Δt used in Table 1), which is mostly independent of the value of n. The use of the tail removal procedure, $\alpha_2(n, \alpha_4)$, results in exactly the same value for this difference in location at t = 2000, except for either n = 3, or $\alpha_4 = 10^{-2}$ and $n \geq 2$, as shown in Table 1. Without the tail removal procedure, the difference between the numerical and analytical compactons after 20000 time steps can be very large, in fact, larger than 26, 3, and 0.8 (in units of space) for $\alpha_4 = 10^{-2}$, 10^{-3} , and 10^{-4} respectively. Hence, Table 1 shows that the tail removal procedure works properly and results in a numerical velocity equal to that of the numerical method without dissipation.

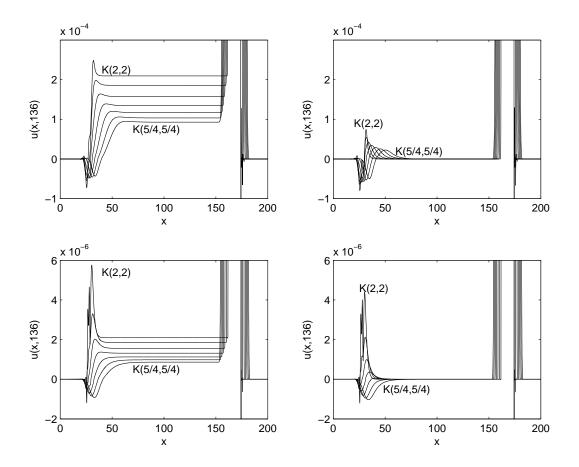


Figure 1: Numerical one-compacton solution of the K(n, n) equation for n = 2, 5/3, 3/2, 7/5, 4/3, 9/7, and 5/4, with $c = 1, c_0 = 0.5, \Delta x = 0.05$, and $\Delta t = 0.04$. The top plots use $\alpha_4 = 10^{-3}$ and the bottom ones $\alpha_4 = 10^{-5}$; the left plots use $\alpha_2 = 0$ and the right ones $\alpha_2(n, \alpha_4)$.

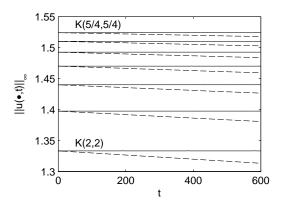


Figure 2: The evolution in time of the maximum amplitude of the one-compacton solution of the K(n, n) equation for n = 2, 5/3, 3/2, 7/5, 4/3, 9/7, and 5/4, with $c = 1, \alpha_4 = 10^{-3}, c_0 = 1, \Delta x = 0.05$, and $\Delta t = 0.04$. The dashed lines use $\alpha_2 = 0$ and the solid ones $\alpha_2(n, \alpha_4)$.

	$\alpha_4 = 10^{-2}$		$\alpha_4 = 10^{-3}$		$\alpha_4 = 10^{-4}$	
n	$\alpha_2 = 0$	$\alpha_2(n, \alpha_4)$	$\alpha_2 = 0$	$\alpha_2(n, \alpha_4)$	$\alpha_2 = 0$	$\alpha_2(n, \alpha_4)$
3	505.50	108.50	53.20	5.50	5.80	0.90
2	404.90	0.90	47.80	0.60	5.40	0.60
5/3	223.10	0.70	25.20	0.60	3.10	0.60
3/2	129.80	0.60	14.40	0.60	2.00	0.60
7/5	80.80	0.60	9.00	0.60	1.40	0.60
4/3	53.20	0.60	6.00	0.60	1.10	0.60
9/7	36.70	0.60	4.20	0.60	0.90	0.60
5/4	26.30	0.60	3.20	0.60	0.80	0.60

Table 1: Difference between the maximum amplitude location of the analytical and numerical one-compacton solutions at time t = 2000 for $\alpha_4 = 10^{-2}$, 10^{-3} , and 10^{-4} , with $\alpha_2 = 0$ and $\alpha_2(n, \alpha_4)$. In this table, c = 1.0, $c_0 = 0.5$, $\Delta x = 0.1$, and $\Delta t = 0.1$ have been used.

4.2. Compacton collisions

The numerical simulation of compacton collisions requires the use of artificial viscosity in order to avoid the appearance of instabilities. It seems that the tail removal procedure introduced in this paper may affect the stability of the simulations for colliding compactons since the explicit artificial viscosity terms has been canceled. Let us summarize our extensive set of simulations showing this is not the case.

Figure 3 illustrates the collision of two compactons of the K(5/3, 5/3) equation with velocities $c_1 = 1.0$, the tallest one, and $c_2 = 0.5$. The upper left plot shows both compactons before the collision. Two snapshots of the collision are presented in the upper right and the lower left plots. Finally, the lower right plot indicates that both compactons recover their amplitude and velocities, but a small ripple remains at the location of the interaction. This collision is typical for all the K(n, n) equations.

Figure 4 shows a zoom in of the numerical simulation of the collision between two compactons of the K(2, 2) equation. The initial positions of the compactons and their velocities ($c_1 = 1$, $c_2 = 0.5$ and $c_0 = 0.1$) have been selected in order to ensure that the fronts of the tail of each compacton are far away at the time of collision. Left plots show both compactons for $\alpha_0 = 0$, before (top plot) and after (middle and bottom ones) their collision. The amplitude of the tail of each compacton depends only on the value of α_4 (equal to 10^{-3} in this figure) when the tails are well separated (see upper left plot in Figure 4), but when the fastest compacton gets to the trailing tail of the slowest, the tail of this second one rides over that of the first one (see middle left plot). As it is widely known in compacton literature [1, 12, 13, 30], a ripple appears after the collision which can be seen around x = 500 in the lower left plot; the ripple amplitude is about two orders of magnitude larger than that of the tails.

The application of the tail removal procedure cancels the trailing tails without affecting the stability of the numerical method during the collision of the compactons, as illustrated in the right plots shown in Fig. 4 for the K(2, 2) equation. The small ripples located at the front of the tails which is not removed by taking $\alpha_2(n, \alpha_4)$ (see upper right plot) do not affect the collision which occurs as if they were absent. Lower right plot illustrates that the compactons, the ripple associated to the collision, and those associated to the tails behave as compactly supported solutions (except for the numerically induced, self-similar, backward and forward radiations reported by Rus and Villatoro [31], whose amplitude is smaller than 10^{-6} in the plots of Fig. 4).

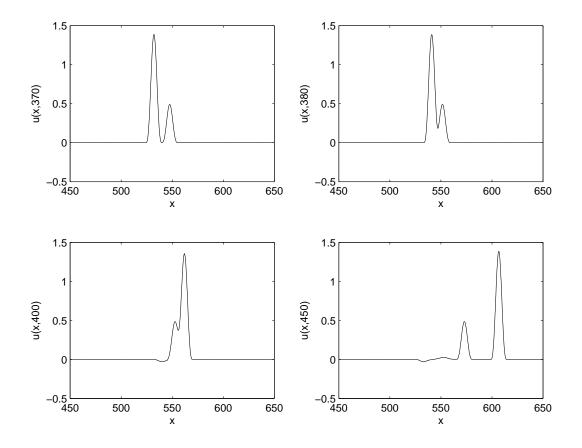


Figure 3: Four snapshots of the collision of two compactons of the K(5/3, 5/3) equation with velocities $c_1 = 1.0$ and $c_2 = 0.5$ at times t = 370, 380, 400, and 450, from upper left to lower right. The parameters used in this simulation are $\alpha_2 = 0$, $\alpha_4 = 10^{-3}$, $c_0 = 0.1$, $\Delta x = 0.1$, and $\Delta t = 0.1$.

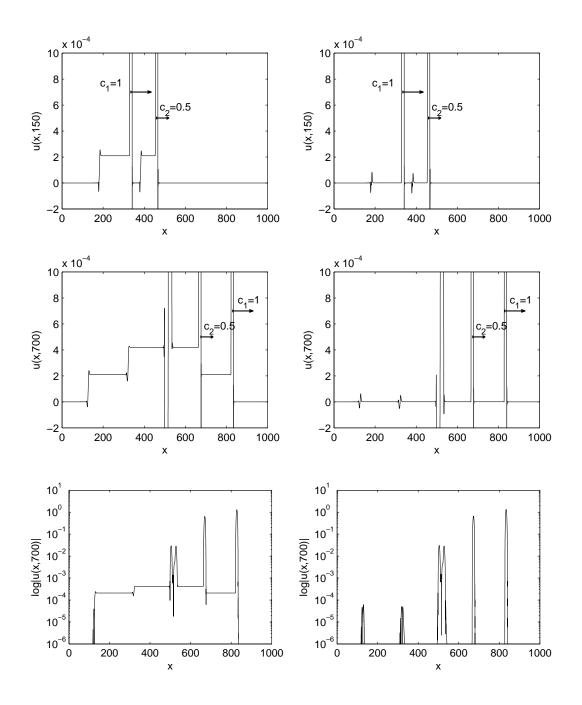


Figure 4: Numerical simulation of two colliding compactons of the K(2,2) equation with velocities $c_1 = 1.0$ and $c_2 = 0.5$ before (top plots with t = 150) and after (middle and bottom ones with t = 700) their mutual collision, with $\alpha_2 = 0$ (left plots) and $\alpha_2(n, \alpha_4)$ (right ones). The parameters used in this simulation are $\alpha_4 = 10^{-3}$, $c_0 = 0.1$, $\Delta x = 0.1$, and $\Delta t = 0.1$. 12

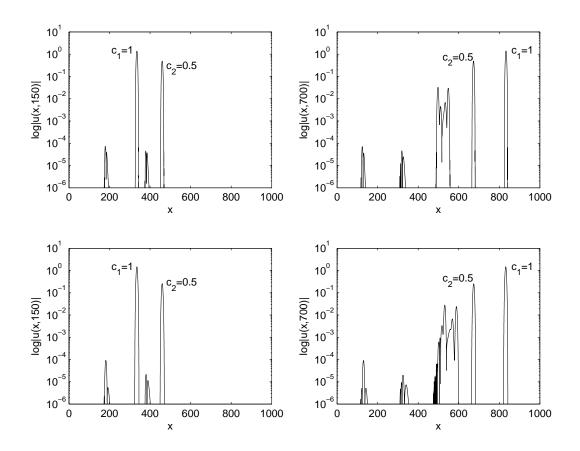


Figure 5: Numerical simulation of two colliding compactons of the K(5/3, 5/3) (top plots) and K(7/5, 7/5) (bottom ones) equations with velocities $c_1 = 1.0$ and $c_2 = 0.5$ before (left plots) and after (right ones) their mutual collision, with $\alpha_2(n, \alpha_4)$. The parameters used in this simulation are $\alpha_4 = 10^{-3}$, $c_0 = 0.1$, $\Delta x = 0.1$, and $\Delta t = 0.1$.

The results shown in Figure 4 for the K(2, 2) equation are representative of an extensive set of simulations of compactons collisions for $n \in \{3, 2, 5/3, 3/2, 7/5, 4/3, 9/7, 5/4\}$, different values of α_4 , c_1 , c_2 , c_0 , Δx , and Δt . Figure 5 shows representative results for the K(5/3, 5/3) (top plots) and K(7/5, 7/5)(bottom ones) equations. The slowest compacton has been stopped by using c_0 and the plots show that the tails have been removed, except for the ripple at their fronts, which are two orders of magnitude smaller than the residual after the collision of the compactons. Further results for other values of nare omitted here for the sake of brevity. In all the cases the proper behavior of the tail removal procedure has been observed.

In long-time integrations, using periodic boundary conditions, two compactons collide multiple times and their trailing tails ride over one another increasing their total amplitude. In such simulations, the value of the artificial viscosity α_4 must be chosen properly in order to avoid the appearance of instabilities resulting in the sudden blow-up of the solution inside the time integration interval. Our results show that the tail removal procedure do not affect the time of blow-up, validating its good performance in terms of the preservation of the stability of the numerical scheme.

5. Conclusions

A procedure for trailing tail removal for numerical methods for the K(n, n) equation incorporating artificial viscosity has been introduced. This procedure is based on the analysis of the effect of the artificial viscosity in the propagation of compactons by means of the adiabatic perturbation method. The performance of the new procedure is illustrated by using a widely used numerical method based on Padé approximants (which also can be derived from finite element and finite difference formulations). The results obtained after an extensive set of simulations show the effectiveness of new the trailing tail removal in the propagation of solutions with both only one compacton and two compactons in mutual interaction.

The new procedure could be applied to other numerical schemes for the K(n, n) equation and for the numerical study of other nonlinear evolution equations presenting compactly supported solutions, such as those with cosine/sine compactors reported in Ref. [32].

Acknowledgements

The authors would like to thank the anonymous reviewers for their valuable comments and suggestions to improve the quality of the paper. The research reported here has been partially supported by Projects MTM2010– 19969, TIN2008–05941 of the Ministerio de Ciencia e Innovación of Spain, and TIC-6083 of the Junta de Andalucía of Spain.

References

- P. Rosenau, J.M. Hyman, Compactons: Solitons with finite wavelength, Phys. Rev. Lett. 70 (1993) 564–567.
- [2] P.J. Olver, P. Rosenau, Tri-Hamiltonian duality between solitons and solitary-wave solutions having compact support, Phys. Rev. E 53 (1996) 1900–1906.
- [3] P. Rosenau, On solitons, compactons, and Lagrange maps, Phys. Lett. A 211 (1996) 265–275.
- [4] Y.A. Li, P.J. Olver, Convergence of solitary-wave solutions in a perturbed bi-Hamiltonian dynamical system. I. Compactons and peakons, Discrete Cont. Dyn. Syst. 3 (1997) 419–432.
- [5] Y.A. Li, P.J. Olver, Convergence of solitary-wave solutions in a perturbed bi-Hamiltonian dynamical system. II. Complex analytic behavior and convergence to non-analytic solutions, Discrete Cont. Dyn. Syst. 4 (1998) 159–191.
- [6] P. Rosenau, Compact and noncompact dispersive patterns, Discrete Cont. Dyn. Syst. 275 (2000) 193–203.
- [7] 2007, V.A. Galaktionov, S.R. Svirshchevskii, Exact Solutions and Invariant Subspaces of Nonlinear Partial Differential Equations in Mechanics and Physics, Chapman & Hall/CRC, Boca Raton, FL.
- [8] V.A. Galaktionov, S.I. Pohozaev, Third-Order Nonlinear Dispersive Equations: Shocks, Rarefaction, and Blowup Waves, Comput. Math. Math. Phys. 48 (2008) 1784–1810.

- [9] D.M. Ambrose, J.D. Wright, Preservation of support and positivity for solutions of degenerate evolution equations, Nonlinearity 23 (2010) 607– 620.
- [10] J.M. Hyman, P. Rosenau, Pulsating multiplet solutions of quintic wave equations, Physica D 123 (1998) 502–512.
- [11] M.S. Ismail, T.R. Taha, A numerical study of compactons, Math. Comput. Simul. 47 (1998) 519–530.
- [12] J. Garralón, F. Rus, F.R. Villatoro, Compacton numerically-induced radiation in a fourth-order finite element method, WSEAS Trans. Math. 5 (2006) 89–96.
- [13] J. de Frutos, M.A. López-Marcos, J.M. Sanz-Serna, A finite difference scheme for the K(2,2) compacton equation, J. Comput. Phys. 120 (1995) 248–252.
- [14] F. Rus, F.R. Villatoro, Padé numerical method for the Rosenau–Hyman compacton equation, Math. Comput. Simul. 76 (2007) 188–192.
- [15] B. Mihaila, A. Cardenas, F. Cooper, A. Saxena, Stability and dynamical properties of Rosenau–Hyman compactons using Padé approximants, Phys. Rev. E 81 (2010) 056708.
- [16] F. Rus, F.R. Villatoro, Numerical methods based on modified equations for nonlinear evolution equations with compactons, Appl. Math. Comput. 204 (2008) 416–422.
- [17] A. Chertock, D. Levy, Particle methods for dispersive equations, J. Comput. Phys. 171 (2001) 708–730.
- [18] F.R. Villatoro, J.I. Ramos, On the method of modified equations. I–V, Appl. Math. Comput. 103 (1999) 111–285.
- [19] J.K. Kevorkian, J.D. Cole, Multiple Scale and Singular Perturbation Methods, Springer, New York, 1996.
- [20] M. Junk, Z.X. Yang, Asymptotic analysis of finite difference methods, Appl. Math. Comput. 158 (2004) 267–301.

- [21] R.L. Herman, C.J. Knickerbocker, Numerically Induced Phase Shift in the KdV Soliton, J. Comput. Phys. 104 (1993) 50–55.
- [22] T.R. Marchant, N.F. Smyth, Soliton interaction for the extended Korteweg-de Vries equation, IMA J. Appl. Math. 55 (1996) 157–176.
- [23] T.R. Marchant, Numerical solitary wave interaction: The order of the inelastic effect, ANZIAM J. 44 (2002) 95–102.
- [24] J. Garralón, F.R. Villatoro, Dissipative perturbations for the K(n, n)Rosenau-Hyman equation, Commun. Nonlinear Sci. Numer. Simul. 17 (2012) 4642-4648.
- [25] A. Pikovsky, P. Rosenau, Phase compactons, Physica D 218 (2006) 56– 69.
- [26] F. Rus, F.R. Villatoro, Adiabatic perturbations for compactons under dissipation and numerically-induced dissipation, J. Comput. Phys. 228 (2009) 4291–4302.
- [27] J.-C. Fernandez, C. Froeschle, G. Reinisch, Adiabatic perturbation of solitons and shock waves, Phys. Scr. 20 (1979) 545–551.
- [28] G.L. Lamb, Elements of Soliton Theory, John Wiley & Sons, 1980.
- [29] L. Girgis, A. Biswas, Soliton perturbation theory for nonlinear wave equations, Appl. Math. Comput. 216 (2010) 2226–2231.
- [30] A. Cardenas, B. Mihaila, F. Cooper, A. Saxena, Properties of compacton-anticompacton collision, Phys. Rev. E 83 (2011) 066705.
- [31] F. Rus, F.R. Villatoro, Self-similar radiation from numerical Rosenau– Hyman compactons, J. Comput. Phys. 227 (2007) 440–454.
- [32] F. Rus, F.R. Villatoro, A repository of equations with cosine/sine compactons, Appl. Math. Comput. 215 (2009) 1838–1851.